Research Article

Gabriel R. Barrenechea, Michał Bosy*, Victorita Dolean, Frédéric Nataf and Pierre-Henri Tournier

Hybrid Discontinuous Galerkin Discretisation and Domain Decomposition Preconditioners for the Stokes Problem

https://doi.org/10.1515/cmam-2018-0005
Received September 6, 2017; revised February 2, 2018; accepted February 28, 2018

Abstract: Solving the Stokes equation by an optimal domain decomposition method derived algebraically involves the use of nonstandard interface conditions whose discretisation is not trivial. For this reason the use of approximation methods such as hybrid discontinuous Galerkin appears as an appropriate strategy: on the one hand they provide the best compromise in terms of the number of degrees of freedom in between standard continuous and discontinuous Galerkin methods, and on the other hand the degrees of freedom used in the nonstandard interface conditions are naturally defined at the boundary between elements. In this paper, we introduce the coupling between a well chosen discretisation method (hybrid discontinuous Galerkin) and a novel and efficient domain decomposition method to solve the Stokes system. We present the detailed analysis of the hybrid discontinuous Galerkin method for the Stokes problem with nonstandard boundary conditions. The full stability and convergence analysis of the discretisation method is presented, and the results are corroborated by numerical experiments. In addition, the advantage of the new preconditioners over more classical choices is also supported by numerical experiments.

Keywords: Stokes Problem, Hybrid Discontinuous Galerkin Methods, Domain Decomposition, Restricted Additive Schwarz Methods

MSC 2010: 65F10, 65N22, 65N30, 65N55

1 Introduction

Discontinuous Galerkin (DG) methods have been first introduced in the early 1970s [25] and they have benefited of a wide interest from the scientific community. The main advantages of these methods are their generality and flexibility as they can be used for a variety of partial differential equations on unstructured meshes. Moreover, they can preserve local properties such as mass and momentum conservation while ensuring a high-order accuracy. However, the cost of these advantages is a larger amount of degrees of freedom in comparison to the continuous Galerkin methods [17] for the same approximation order.

Gabriel R. Barrenechea, Department of Mathematics and Statistics, University of Strathclyde, 26 Richmond Street, G1 1XH Glasgow, United Kingdom, e-mail: gabriel.barrenechea@strath.ac.uk
***Corresponding author: Michał Bosy,** Department of Mathematics and Statistics, University of Strathclyde, 26 Richmond Street, G1 1XH Glasgow, United Kingdom, e-mail: michal.bosy@unipv.it. http://orcid.org/0000-0003-2723-6913
Victorita Dolean, Department of Mathematics and Statistics, University of Strathclyde, 26 Richmond Street, G1 1XH Glasgow, United Kingdom, and Faculté des Sciences, University Côte d'Azur, Lab. J-A Dieudonné, Parc Valrose, 06108 Nice Cedex 02, France, e-mail: victorita.dolean@strath.ac.uk. http://orcid.org/0000-0002-5885-1903
Frédéric Nataf, Pierre-Henri Tournier, CNRS, INRIA, Laboratoire Jacques-Louis Lions, Sorbonne Université, Université Paris-Diderot SPC, équipe Alpines, 75005 Paris, France, e-mail: nataf@ann.jussieu.fr, tournier@ljll.math.upmc.fr

A good compromise between the previous methods, while preserving the high order, are the hybridised versions of DG using divergence conforming spaces such as Raviart–Thomas (RT) and Brezzi–Douglas–Marini (BDM) [2]. These methods are a subset of the hybrid discontinuous Galerkin (HDG) methods, introduced in [8] for second-order elliptic problems, and extended to three-dimensional Stokes equation in [7]. The authors present there the mixed formulation of HDG methods defined locally on each element. They consider many types of boundary conditions that involve normal and tangential velocity, pressure, and tangential stress. The formulations of the methods are similar, the only difference lies in the choice of the numerical traces. A refined analysis of HDG methods for the Stokes equation with Dirichlet boundary conditions was presented in [9], where optimal convergence in the HDG norm is proven, and superconvergent postprocessings are introduced. An alternative strategy to approximate the Stokes problem was used in [16], where a combination of HDG and a symmetric interior penalty (somehow linked to the work [27]) is presented and analysed.

In a further paper [15] this approach is extended to Darcy, and coupled Darcy–Stokes flows. The new formulation includes different degrees of polynomials for finite element spaces associated with different variables.

In all HDG discretisations, one important component is the Lagrange multiplier defined on the inter element edges (faces in 3D). In the work [22] the authors approximate the Navier–Stokes equation using $H(\mathrm{div})$-conforming spaces (rather than the usual H^1-conforming ones) together with an HDG approach. Now, in order to reduce the number of degrees of freedom needed for the Lagrange multiplier, the authors introduce an edge-wise projection into a finite element space of lower degree. This projection was also shown to be of paramount importance to establish the connection between the hybrid high-order [11] and the HDG methods presented in [6].

Even considering the decrease of the number of degrees of freedom provided by the HDG methods with projection, modern applications lead to linear systems whose size is too large to allow the use of direct solvers. Thus, parallel solvers are becoming increasingly important in scientific computing. A natural paradigm to take advantage of modern parallel architectures is the Domain Decomposition method, see e.g. [12, 24, 28, 31]. Domain decomposition methods are iterative solvers based on a decomposition of a global domain into subdomains. At each iteration, one (or two) boundary value problem(s) are solved in each subdomain and the continuity of the solution at the interfaces between subdomains is only satisfied at convergence of the iterative procedure. The partial differential equation is the one of the global problem.

For Additive Schwarz methods and Schur complement methods, the boundary conditions on the interfaces between subdomains, or, interface conditions (IC), are Dirichlet or Neumann boundary conditions. For scalar equations there is a consensus on this choice of IC. On the other hand, for systems of differential equations, such as the Stokes or incompressible elasticity equations, alternatives like normal velocity-tangential flux (NVTF) or tangential velocity-normal flux (TVNF) IC should be superior to the pure velocity (Dirichlet like) or pure stress (Neumann like) IC, see [12, Section 6.6] and the references therein. In [19], this choice was motivated by symmetry considerations, while in [4, 5, 14], they were obtained by an analysis of the systems of partial differential equations by symbolic techniques, mostly linked to the Smith factorization [29]. Similar attempts to derive more intrinsic IC to the nature of the equation to solve were derived [13] for the Euler system.

Due to the difficulty of implementing these IC, previous numerical tests were restricted to decompositions where the boundaries of subdomains are rectilinear so that the normal to the interface is easy to define. The underlying domain decomposition method was a Schur complement method. That is mainly the reason we have considered and analysed a specific HDG method where this kind of degrees of freedom are naturally present.

In this paper, we want to combine appropriate HDG discretisation and the associated domain decomposition methods mentioned above using nonstandard IC. The combination of the two is meant to provide a competitive solving strategy for this kind of partial differential equation system. A different, but somewhat related, approach can be found in [1] where a DG type discretisation is coupled to a discrete Helmholtz decomposition to propose some preconditioners.

Concerning the HDG discretisation, in approach similar to the one presented in this work, but using completely discontinuous spaces, is given in [23]. Our analysis is related to the one in that paper, but the method

presented herein uses $H(\mathrm{div})$-conforming spaces, which implies in turn that the Lagrange multipliers are scalar valued. The combination of these two facts reduces the number of degrees of freedom significantly. In addition, the use of nonstandard boundary conditions (motivated by the newly defined domain decomposition preconditioners) makes the analysis somehow more involved.

The rest of the paper is organised as follows. To start with, we introduce the problem and notation in Section 2. In Section 3, we present the hybridisation of a symmetric interior penalty Galerkin method that allows us to impose the TVNF and NVTF boundary conditions in quite a natural way. The formulation is similar to the one from [22] with Dirichlet boundary conditions. In addition to different kinds of boundary conditions, we include a local edge-based projection in order to reduce the dimension of the space of Lagrange multipliers. Our analysis follows the one from [22] (see also [21] for a more detailed version). Thanks to the HDG discretisation, we can consider domain decomposition methods with arbitrary shape of the interfaces and Schwarz type methods. In Section 4, the Additive Schwarz methods are defined at the algebraic level. Section 5 contains the numerical results, including the convergence validation of the HDG method and a comparison of the domain decomposition preconditioners. Finally, some conclusions are drawn.

2 Notation and Preliminary Results

Let Ω be an open polygonal domain in $\mathbb{R}^2$ with Lipschitz boundary $\Gamma := \partial\Omega$. We use boldface font for tensor or vector variables, e.g. $\boldsymbol{u}$ is a velocity vector field. The scalar variables will be italic, e.g. p denotes a pressure scalar value. We define the stress tensor $\boldsymbol{\sigma} := \nu\nabla\boldsymbol{u} - p\boldsymbol{I}$ and the flux $\boldsymbol{\sigma_n} := \boldsymbol{\sigma}\boldsymbol{n}$. In addition, we denote normal and tangential components as follows: $u_n := \boldsymbol{u}\cdot\boldsymbol{n}$, $u_t := \boldsymbol{u}\cdot\boldsymbol{t}$, $\sigma_{nn} := \boldsymbol{\sigma_n}\cdot\boldsymbol{n}$, $\sigma_{nt} := \boldsymbol{\sigma_n}\cdot\boldsymbol{t}$, where $\boldsymbol{n}$ is the outward unit normal vector to the boundary Γ and $\boldsymbol{t}$ is a vector tangential to Γ such that $\boldsymbol{n}\cdot\boldsymbol{t} = 0$.

For $D \subset \Omega$, we use the standard $L^2(D)$ space with the following norm:

$$\|f\|_D^2 := \int_D f^2\, d\boldsymbol{x} \quad \text{for all } f \in L^2(D).$$

Let us define, for $m \in \mathbb{N}$, the following Sobolev spaces:

$$H^m(D) := \{v \in L^2(D) : \partial^{\boldsymbol{\alpha}} v \in L^2(D) \text{ for all } |\boldsymbol{\alpha}| \le m\},$$
$$H(\mathrm{div}, D) := \{\boldsymbol{v} \in [L^2(D)]^2 : \nabla\cdot\boldsymbol{v} \in L^2(D)\},$$

where, for $\boldsymbol{\alpha} = (\alpha_1, \alpha_2) \in \mathbb{N}^2$, $|\boldsymbol{\alpha}| = \alpha_1 + \alpha_2$, and

$$\partial^{\boldsymbol{\alpha}} = \frac{\partial^{|\boldsymbol{\alpha}|}}{\partial x_1^{\alpha_1}\partial x_2^{\alpha_2}}.$$

In addition, we will use following standard semi-norm and norm for the Sobolev space $H^m(D)$:

$$|f|_{H^m(D)}^2 := \sum_{|\boldsymbol{\alpha}|=m} \|\partial^{\boldsymbol{\alpha}} f\|_D^2, \quad \|f\|_{H^m(D)}^2 := \sum_{k=0}^{m} |f|_{H^k(D)}^2 \quad \text{for all } f \in H^m(D).$$

In this work, we consider the two-dimensional Stokes problem

$$\begin{cases} -\nu\Delta\boldsymbol{u} + \nabla p = \boldsymbol{f} & \text{in } \Omega, \\ \nabla\cdot\boldsymbol{u} = 0 & \text{in } \Omega, \end{cases} \tag{2.1}$$

where $\boldsymbol{u} : \bar{\Omega} \to \mathbb{R}^2$ is the unknown velocity field, $p : \bar{\Omega} \to \mathbb{R}$ the pressure, $\nu > 0$ the viscosity, which is considered to be constant, and $\boldsymbol{f} \in [L^2(\Omega)]^2$ is a given function. For $g \in L^2(\Gamma)$ we consider two types of boundary conditions:

- tangential-velocity and normal-flux (TVNF)

$$\begin{cases} \sigma_{nn} = g & \text{on } \Gamma, \\ u_t = 0 & \text{on } \Gamma, \end{cases} \tag{2.2}$$

- normal-velocity and tangential-flux (NVTF)

$$\begin{cases} \sigma_{nt} = g & \text{on } \Gamma, \\ u_n = 0 & \text{on } \Gamma, \end{cases} \tag{2.3}$$

which together with (2.1) define two boundary value problems. We will detail the analysis for the TVNF boundary value problem

$$\begin{cases} -\nu\Delta \boldsymbol{u} + \nabla p = \boldsymbol{f} & \text{in } \Omega, \\ \nabla \cdot \boldsymbol{u} = 0 & \text{in } \Omega, \\ \sigma_{nn} = g & \text{on } \Gamma, \\ u_t = 0 & \text{on } \Gamma, \end{cases} \tag{2.4}$$

since considering the NVTF boundary conditions (2.3) instead is very similar. We will just add a remark when necessary to stress the differences between them. The restriction to homogeneous Dirichlet conditions on u_t is made only to simplify the presentation.

Let $\{\mathcal{T}_h\}_{h>0}$ be a regular family of triangulations of $\bar{\Omega}$ made of triangles. For each triangulation $\mathcal{T}_h$, $\mathcal{E}_h$ denotes the set of its edges. In addition, we set $h_K := \operatorname{diam}(K)$ for each $K \in \mathcal{T}_h$, and $h := \max_{K\in\mathcal{T}_h} h_K$. We define the following Sobolev spaces on the triangulation $\mathcal{T}_h$ and the set of all edges in $\mathcal{E}_h$:

$$L^2(\mathcal{E}_h) := \{v : v|_E \in L^2(E) \text{ for all } E \in \mathcal{E}_h\},$$
$$H^m(\mathcal{T}_h) := \{v \in L^2(\Omega) : v|_K \in H^m(K) \text{ for all } K \in \mathcal{T}_h\} \quad \text{for } m \in \mathbb{N},$$

with the corresponding broken norms.

The following results will be very useful in what follows.

Lemma 2.1 (Inverse and Trace Inequalities). *There exist C, $C_{\max} > 0$, independent of h_K, such that for every $K \in \mathcal{T}_h$ and every polynomial function v in K the following inequalities hold:*

$$|v|_{H^s(K)} \le C h_K^{m-s} |v|_{H^m(K)}, \quad 0 \le m \le s, \tag{2.5}$$

$$h_K^{\frac{1}{2}} \|v\|_{\partial K} \le C_{\max} \|v\|_K. \tag{2.6}$$

Moreover, there exists $C > 0$, independent of h_K, such that for any $v \in H^1(K)$, the following local trace inequality holds:

$$\|v\|_{\partial K} \le C\left(h_K^{-\frac{1}{2}} \|v\|_K + h_K^{\frac{1}{2}} |v|_{H^1(K)}\right). \tag{2.7}$$

Proof. For (2.5) see [17, Lemma 1.138] and for (2.6) see [10, Lemma 1.46]. The discrete trace inequality (2.7) follows by standard scaling arguments. □

We now introduce the finite element spaces used for discretisation. First, we present them for the particular case in which we consider the TVNF boundary condition. For this case for $k \ge 1$, we discretise the velocity using the Brezzi–Douglas–Marini space (see [2, Section 2.3.1]) given by

$$\mathrm{BDM}_h^k := \{\boldsymbol{v_h} \in H(\operatorname{div}, \Omega) : \boldsymbol{v_h}|_K \in [\mathbb{P}_k(K)]^2 \text{ for all } K \in \mathcal{T}_h\}.$$

The choice of the above finite element spaces is motivated by two requirements. On the one hand, we have imposed that the finite element space must be conforming in $H(\operatorname{div}, \Omega)$, while on the other hand, it has to satisfy the inf-sup condition with respect to a broken H^1-norm of the velocity. The BDM space appears then as a natural alternative satisfying both these requirements. In fact, other popular alternatives, such as the Raviart–Thomas space, while conforming in $H(\operatorname{div}, \Omega)$ do not satisfy the inf-sup condition with respect to the norm used in this work.

In addition, for $1 \le m \le k+1$ we denote by $\Pi^k : [H^m(\Omega)]^2 \to \mathrm{BDM}_h^k$ the BDM projection defined in [2, Section 2.5]. The HDG formulation includes a Lagrange multiplier over the internal edges. In order to propose a discretisation with fewer degrees of freedom, we discretise the Lagrange multiplier $\tilde{u}$ using the spaces

$$M_h^{k-1} := \{\tilde{v}_h \in L^2(\mathcal{E}_h) : \tilde{v}_h|_E \in \mathbb{P}_{k-1}(E) \text{ for all } E \in \mathcal{E}_h\},$$
$$M_{h,0}^{k-1} := \{\tilde{v}_h \in M_h^{k-1} : \tilde{v}_h = 0 \text{ on } \Gamma\}.$$

Furthermore, we introduce for all $E \in \mathcal{E}_h$ the $L^2(E)$-projection $\Phi_E^{k-1} : L^2(E) \to \mathbb{P}_{k-1}(E)$ defined as follows. For every $\tilde{w} \in L^2(E)$, $\Phi_E^{k-1}(\tilde{w})$ is the unique element of $\mathbb{P}_{k-1}(E)$ satisfying

$$\int_E \Phi_E^{k-1}(\tilde{w})\tilde{v}_h \, ds = \int_E \tilde{w}\tilde{v}_h \, ds \quad \text{for all } \tilde{v}_h \in \mathbb{P}_{k-1}(E),$$

and we define $\Phi^{k-1} : L^2(\mathcal{E}_h) \to M_h^{k-1}$ by $\Phi^{k-1}|_E := \Phi_E^{k-1}$ for all $E \in \mathcal{E}_h$.

Let us denote $\boldsymbol{V_h} := \mathrm{BDM}_h^k \times M_{h,0}^{k-1}$. The pressure is discretised using the following space:

$$Q_h^{k-1} := \{q_h \in L^2(\Omega) : q_h|_K \in \mathbb{P}_{k-1}(K) \text{ for all } K \in \mathcal{T}_h\}.$$

In addition, we define the local $L^2(K)$-projection $\Psi_K^{k-1} : L^2(K) \to \mathbb{P}_{k-1}(K)$ for each $K \in \mathcal{T}_h$ defined as follows. For every $w \in L^2(K)$, $\Psi_K^k(w)$ is the unique element of $\mathbb{P}_{k-1}(K)$ satisfying

$$\int_K \Psi_K^{k-1}(w)v_h dx = \int_K w v_h dx \quad \text{for all } v_h \in \mathbb{P}_{k-1}(K).$$

We will also use the following results.

Lemma 2.2 (Approximation Results). *There exists $C > 0$, independent of h_K, such that for all $\boldsymbol{v} \in [H^m(K)]^2$ and $v \in H^m(K)$, $1 \le m \le k+1$, the following interpolation estimates hold:*

- *local Brezzi–Douglas–Marini approximation*

$$\|\boldsymbol{v} - \Pi^k(\boldsymbol{v})\|_K \le Ch_K^m |\boldsymbol{v}|_{H^m(K)}, \quad \|\boldsymbol{v} - \Pi^k(\boldsymbol{v})\|_{H^1(K)} \le Ch_K^{m-1} |\boldsymbol{v}|_{H^m(K)}, \tag{2.8}$$

- *trace L^2-projection approximation*

$$\|v - \Phi^k(v)\|_{\partial K} \le Ch_K^{m-\frac{1}{2}} |v|_{H^m(K)}, \tag{2.9}$$

- *local L^2-projection approximation*

$$\|v - \Psi_K^k(v)\|_K \le Ch_K^m |v|_{H^m(K)}, \quad |v - \Psi_K^k(v)|_{H^1(K)} \le Ch_K^{m-1} |v|_{H^m(K)}. \tag{2.10}$$

Proof. For (2.8) see [2, Proposition 2.5.1], for (2.9) see [18, Lemma III.2.10], and for (2.10) see the proof of [17, Theorem 1.103]. □

3 Hybrid Discontinuous Galerkin Method

In this section, we introduce the HDG method proposed in this work, study its well-posedness, and analyse its error.

3.1 The Discrete Problem

From now on we will use ∇ to denote the element-wise gradient. First, we multiply the first equation from (2.1) by a test function $\boldsymbol{v_h} \in \mathrm{BDM}_h^k$ and integrate by parts. This gives

$$\int_\Omega (-\nu\Delta\boldsymbol{u} + \nabla p) \cdot \boldsymbol{v_h} \, d\boldsymbol{x} = \sum_{K \in \mathcal{T}_h} \Big(\int_K \nu\nabla\boldsymbol{u} : \nabla\boldsymbol{v_h} \, d\boldsymbol{x} - \int_K p\nabla \cdot \boldsymbol{v_h} \, d\boldsymbol{x} - \int_{\partial K} \nu\boldsymbol{\partial_n u}\boldsymbol{v_h} \, ds + \int_{\partial K} p(\boldsymbol{v_h})_n \, ds \Big). \tag{3.1}$$

Since the normal and tangential vectors are perpendicular ($\boldsymbol{n} \cdot \boldsymbol{t} = 0$), we can split (3.1) as

$$\int_\Omega (-\nu\Delta\boldsymbol{u} + \nabla p) \cdot \boldsymbol{v_h} \, d\boldsymbol{x} = \sum_{K \in \mathcal{T}_h} \Big(\int_K \nu\nabla\boldsymbol{u} : \nabla\boldsymbol{v_h} \, d\boldsymbol{x} - \int_K p\nabla \cdot \boldsymbol{v_h} \, d\boldsymbol{x} - \int_{\partial K} \sigma_{nt}(\boldsymbol{v_h})_t \, ds - \int_{\partial K} \sigma_{nn}(\boldsymbol{v_h})_n \, ds \Big). \tag{3.2}$$

For the solution of the Stokes problem (2.1), $\boldsymbol{\sigma_n}$ is continuous across all interior edges. Moreover, since $\boldsymbol{v_h} \in \mathrm{BDM}_h^k$, we see that $(\boldsymbol{v_h})_n$ is continuous across all interior edges, and thus we can rewrite (3.2) as

$$\int_\Omega (-\nu\Delta\boldsymbol{u} + \nabla p)\cdot\boldsymbol{v_h}\,d\boldsymbol{x} = \sum_{K\in\mathcal{T}_h}\Big(\int_K \nu\nabla\boldsymbol{u} : \nabla\boldsymbol{v_h}\,d\boldsymbol{x} - \int_K p\nabla\cdot\boldsymbol{v_h}\,d\boldsymbol{x} - \int_{\partial K}\sigma_{nt}(\boldsymbol{v_h})_t\,ds\Big) - \int_\Gamma \sigma_{nn}(\boldsymbol{v_h})_n\,ds. \tag{3.3}$$

In addition, since $\boldsymbol{\sigma_n}$ is continuous across all interior edges, we have

$$\sum_{K\in\mathcal{T}_h}\int_{\partial K}\sigma_{nt}\tilde{v}_h\,ds = 0 \quad \text{for all } \tilde{v}_h \in M_{h,0}^{k-1},$$

and we can add this to (3.3) to get

$$\int_\Omega (-\nu\Delta\boldsymbol{u} + \nabla p)\cdot\boldsymbol{v_h}\,d\boldsymbol{x} = \sum_{K\in\mathcal{T}_h}\Big(\int_K \nu\nabla\boldsymbol{u} : \nabla\boldsymbol{v_h}\,d\boldsymbol{x} - \int_K p\nabla\cdot\boldsymbol{v_h}\,d\boldsymbol{x} - \int_{\partial K}\sigma_{nt}((\boldsymbol{v_h})_t - \tilde{v}_h)\,ds\Big) - \int_\Gamma \sigma_{nn}(\boldsymbol{v_h})_n\,ds. \tag{3.4}$$

Denoting $\tilde{u} = u_t$ on $\mathcal{E}_h$ leads to $(u_t - \tilde{u}) = \Phi^{k-1}(u_t - \tilde{u}) = 0$ on $\mathcal{E}_h$. Applying the boundary conditions (2.2), we can rewrite (3.4) as

$$\begin{aligned}\int_\Omega (-\nu\Delta\boldsymbol{u} + \nabla p)\cdot\boldsymbol{v_h}\,d\boldsymbol{x} = \sum_{K\in\mathcal{T}_h}\Big(&\int_K \nu\nabla\boldsymbol{u} : \nabla\boldsymbol{v_h}\,d\boldsymbol{x} - \int_K p\nabla\cdot\boldsymbol{v_h}\,d\boldsymbol{x}\\ &- \int_{\partial K}\nu(\boldsymbol{\partial_n u})_t((\boldsymbol{v_h})_t - \tilde{v}_h)\,ds \pm \int_{\partial K}\nu(u_t - \tilde{u})(\boldsymbol{\partial_n v_h})_t\,ds\\ &+ \nu\frac{\tau}{h_K}\int_{\partial K}\Phi^{k-1}(u_t - \tilde{u})\Phi^{k-1}((\boldsymbol{v_h})_t - \tilde{v}_h)\,ds\Big) - \int_\Gamma g(\boldsymbol{v_h})_n\,ds,\end{aligned}$$

where $\tau > 0$ is a stabilisation parameter. Hence, we define the velocity bilinear form $a : \boldsymbol{V_h}\times\boldsymbol{V_h} \to \mathbb{R}$ as

$$\begin{aligned}a((\boldsymbol{w_h},\tilde{w}_h),(\boldsymbol{v_h},\tilde{v}_h)) := \sum_{K\in\mathcal{T}_h}\Big(&\int_K \nu\nabla\boldsymbol{w_h} : \nabla\boldsymbol{v_h}\,d\boldsymbol{x} - \int_{\partial K}\nu(\boldsymbol{\partial_n w_h})_t((\boldsymbol{v_h})_t - \tilde{v}_h)\,ds\\ &+ \varepsilon\int_{\partial K}\nu((\boldsymbol{w_h})_t - \tilde{w}_h)(\boldsymbol{\partial_n v_h})_t\,ds\\ &+ \nu\frac{\tau}{h_K}\int_{\partial K}\Phi^{k-1}((\boldsymbol{w_h})_t - \tilde{w}_h)\Phi^{k-1}((\boldsymbol{v_h})_t - \tilde{v}_h)\,ds\Big),\end{aligned} \tag{3.5}$$

where $\varepsilon \in \{-1, 1\}$ and $\tau > 0$ is a stabilisation parameter, and $b : \boldsymbol{V_h}\times Q_h^{k-1} \to \mathbb{R}$ as

$$b((\boldsymbol{v_h},\tilde{v}_h), q_h) := -\sum_{K\in\mathcal{T}_h}\int_K q_h\nabla\cdot\boldsymbol{v_h}\,d\boldsymbol{x}.$$

With these definitions we propose the HDG method for the TVNF boundary value problem (2.4):

Find $(\boldsymbol{u_h},\tilde{u}_h,p_h) \in \boldsymbol{V_h}\times Q_h^{k-1}$ such that for all $(\boldsymbol{v_h},\tilde{v}_h,q_h) \in \boldsymbol{V_h}\times Q_h^{k-1}$,

$$\begin{cases} a((\boldsymbol{u_h},\tilde{u}_h),(\boldsymbol{v_h},\tilde{v}_h)) + b((\boldsymbol{v_h},\tilde{v}_h),p_h) = \displaystyle\int_\Omega \boldsymbol{f}\boldsymbol{v_h}\,d\boldsymbol{x} + \int_\Gamma g(\boldsymbol{v_h})_n\,ds,\\ b((\boldsymbol{u_h},\tilde{u}_h),q_h) = 0.\end{cases} \tag{3.6}$$

Remark 3.1. The use of $H(\mathrm{div})$-conforming spaces not only decreases the number of degrees of freedom in comparison to [23], but leads as well to a simpler bilinear form b, as the jump terms appearing in that reference are no longer needed for stability or consistency.

3.2 Well-Posedness of the Discrete Problem

Let us consider the following semi-norm:

$$|||(\boldsymbol{w_h}, \tilde{w}_h)|||^2 := \nu \sum_{K\in\mathcal{T}_h} \Big(|\boldsymbol{w_h}|^2_{H^1(K)} + h_K \|\boldsymbol{\partial_n w_h}\|^2_{\partial K} + \frac{\tau}{h_K} \|\Phi^{k-1}((\boldsymbol{w_h})_t - \tilde{w}_h)\|^2_{\partial K} \Big). \tag{3.7}$$

Lemma 3.2. *The semi-norm $|||\cdot|||$ defined by* (3.7) *is a norm on $\boldsymbol{V_h}$.*

Proof. Since $|||\cdot|||$ is a semi-norm, we only need to show that

$$|||(\boldsymbol{w_h}, \tilde{w}_h)||| = 0 \quad \Longrightarrow \quad \boldsymbol{w_h} = \boldsymbol{0} \text{ and } \tilde{w}_h = 0.$$

Let us suppose $(\boldsymbol{w_h}, \tilde{w}_h) \in \boldsymbol{V_h}$ and $|||(\boldsymbol{w_h}, \tilde{w}_h)||| = 0$. Then $\nabla \boldsymbol{w_h} = 0$ in all $K \in \mathcal{T}_h$, and thus $\boldsymbol{w_h}|_K = \boldsymbol{C}_K$ for all $K \in \mathcal{T}_h$. Now, since $\boldsymbol{w_h} \in [\mathbb{P}_0(K)]^2$ in every K, we have

$$\|\Phi^{k-1}((\boldsymbol{w_h})_t - \tilde{w}_h)\|_{\partial K} = 0 \quad \Longrightarrow \quad (\boldsymbol{w_h})_t = \tilde{w}_h \text{ in each } E \in \mathcal{E}_h.$$

Since $\tilde{w}_h$ is single valued on all the edges in $\mathcal{E}_h$, we have that $(\boldsymbol{w_h})_t$ is continuous in Ω. Moreover, $\boldsymbol{w_h}$ belongs to BDM^k_h, so $(\boldsymbol{w_h})_n$ is also continuous in Ω. Then, $\boldsymbol{w_h}$ is continuous in Ω, and thus $\boldsymbol{w_h} = \boldsymbol{C} \in \mathbb{R}^2$ in Ω. Finally,

$$(\boldsymbol{w_h})_t = (\boldsymbol{C})_t = 0 \text{ on } \Gamma \quad \Longrightarrow \quad \boldsymbol{w_h} = \boldsymbol{0} \text{ in } \Omega,$$

which finishes the proof since $\tilde{w}_h = (\boldsymbol{w_h})_t$ on every edge. □

Lemma 3.3. *There exists $C > 0$ such that, for all $(\boldsymbol{w}, \tilde{w}), (\boldsymbol{v}, \tilde{v}) \in [H^1(\Omega) \cap H^2(\mathcal{T}_h)]^2 \times L^2(\mathcal{E}_h)$ and $q \in L^2(\Omega)$, we have*

$$|a((\boldsymbol{w}, \tilde{w}), (\boldsymbol{v}, \tilde{v}))| \le C |||(\boldsymbol{w}, \tilde{w})||| \, |||(\boldsymbol{v}, \tilde{v})|||, \tag{3.8}$$

$$|b((\boldsymbol{w}, \tilde{w}), q)| \le \sqrt{\frac{2}{\nu}} \, |||(\boldsymbol{w}, \tilde{w})||| \, \|q\|_\Omega. \tag{3.9}$$

Proof. Let us start with (3.8). Using the Cauchy–Schwarz inequality, we get

$$|a((\boldsymbol{w}, \tilde{w}), (\boldsymbol{v}, \tilde{v}))| \le 2 |||(\boldsymbol{w}, \tilde{w})||| \, |||(\boldsymbol{v}, \tilde{v})||| + \sum_{K\in\mathcal{T}_h} \big(\nu \|\boldsymbol{\partial_n w}\|_{\partial K} \|v_t - \tilde{v}\|_{\partial K} + \nu \|\boldsymbol{\partial_n v}\|_{\partial K} \|w_t - \tilde{w}\|_{\partial K} \big).$$

Therefore, using the triangle inequality and the trace L^2-projection approximation (2.9), we get

$$\begin{aligned} \|\boldsymbol{\partial_n w}\|_{\partial K} \|v_t - \tilde{v}\|_{\partial K} &\le \|\boldsymbol{\partial_n w}\|_{\partial K} \|v_t - \Phi^{k-1}(v_t)\|_{\partial K} + \|\boldsymbol{\partial_n w}\|_{\partial K} \|\Phi^{k-1}(v_t - \tilde{v})\|_{\partial K} \\ &\le \tilde{c}_1 \sqrt{h_K} \|\boldsymbol{\partial_n w}\|_{\partial K} |\boldsymbol{v}|_{H^1(K)} + \|\boldsymbol{\partial_n w}\|_{\partial K} \|\Phi^{k-1}(v_t - \tilde{v})\|_{\partial K}. \end{aligned}$$

Thus, using the Cauchy–Schwarz inequality gives

$$\begin{aligned} \nu \|\boldsymbol{\partial_n w}\|_{\partial K} \|v_t - \tilde{v}\|_{\partial K} &\le c_1 |||(\boldsymbol{w}, \tilde{w})||| \, |||(\boldsymbol{v}, \tilde{v})|||, \\ \nu \|\boldsymbol{\partial_n v}\|_{\partial K} \|w_t - \tilde{w}\|_{\partial K} &\le c_2 |||(\boldsymbol{v}, \tilde{v})||| \, |||(\boldsymbol{w}, \tilde{w})|||. \end{aligned}$$

Finally, we get (3.8) for $C = (2 + c_1 + c_2)$. The continuity (3.9) is analogous. □

To show the well-posedness of (3.6) we need the ellipticity of the bilinear form a and an inf-sup condition for the bilinear form b. We start by showing that a is elliptic with respect to $|||\cdot|||$.

Lemma 3.4. *There exists $\alpha > 0$ such that for all $(\boldsymbol{v_h}, \tilde{v}_h) \in \boldsymbol{V_h}$,*

$$a((\boldsymbol{v_h}, \tilde{v}_h), (\boldsymbol{v_h}, \tilde{v}_h)) \ge \alpha |||(\boldsymbol{v_h}, \tilde{v}_h)|||^2. \tag{3.10}$$

If $\varepsilon = -1$ in the definition (3.5)*, then inequality* (3.10) *only holds under the additional hypothesis of τ being large enough. If $\varepsilon = 1$ in* (3.5)*, then inequality* (3.10) *holds for arbitrary τ.*

Proof. First, since $\boldsymbol{\partial_n v_h}|_E \in [\mathbb{P}_{k-1}(E)]^2$ for all $E \in \mathcal{E}_h$, we have

$$a((\boldsymbol{v_h}, \tilde{v}_h), (\boldsymbol{v_h}, \tilde{v}_h)) = \sum_{K\in\mathcal{T}_h} \Big(\nu|\boldsymbol{v_h}|^2_{H^1(K)} - \nu(1-\varepsilon) \int_{\partial K} (\boldsymbol{\partial_n v_h})_t \Phi^{k-1}((\boldsymbol{v_h})_t - \tilde{v}_h)\, ds + \nu \frac{\tau}{h_K} \|\Phi^{k-1}((\boldsymbol{v_h})_t - \tilde{v}_h)\|^2_{\partial K} \Big). \tag{3.11}$$

To bound the middle term in terms of the other two, we consider two cases.

Case 1: $\varepsilon = 1$. Then (3.11) reduces to

$$a((\boldsymbol{v_h}, \tilde{v}_h), (\boldsymbol{v_h}, \tilde{v}_h)) = \sum_{K\in\mathcal{T}_h} \Big(\nu|\boldsymbol{v_h}|^2_{H^1(K)} + \nu \frac{\tau}{h_K} \|\Phi^{k-1}((\boldsymbol{v_h})_t - \tilde{v}_h)\|^2_{\partial K} \Big). \tag{3.12}$$

It only remains to show that the right-hand side of (3.12) is an upper bound (up to a constant) for the norm $|||\cdot|||$ given by (3.7). Using the discrete trace inequality (2.6), we get

$$\sum_{K\in\mathcal{T}_h} h_K \|\boldsymbol{\partial_n v_h}\|^2_{\partial K} \le \sum_{K\in\mathcal{T}_h} C^2_{\max} |\boldsymbol{v_h}|^2_{H^1(K)},$$

and then

$$|||(\boldsymbol{v_h}, \tilde{v}_h)|||^2 \le (1 + C^2_{\max}) \sum_{K\in\mathcal{T}_h} \nu \Big(|\boldsymbol{v_h}|^2_{H^1(K)} + \frac{\tau}{h_K} \|\Phi^{k-1}((\boldsymbol{v_h})_t - \tilde{v}_h)\|^2_{\partial K} \Big), \tag{3.13}$$

which proves (3.10) with $\alpha = 1/(1 + C^2_{\max})$.

Case 2: $\varepsilon = -1$. Then (3.11) becomes

$$a((\boldsymbol{v_h}, \tilde{v}_h), (\boldsymbol{v_h}, \tilde{v}_h)) = \sum_{K\in\mathcal{T}_h} \Big(\nu|\boldsymbol{v_h}|^2_{H^1(K)} - 2\nu \int_{\partial K} (\boldsymbol{\partial_n v_h})_t \Phi^{k-1}((\boldsymbol{v_h})_t - \tilde{v}_h)\, ds + \nu \frac{\tau}{h_K} \|\Phi^{k-1}((\boldsymbol{v_h})_t - \tilde{v}_h)\|^2_{\partial K} \Big).$$

Using the Cauchy–Schwarz inequality, we deduce

$$a((\boldsymbol{v_h}, \tilde{v}_h), (\boldsymbol{v_h}, \tilde{v}_h)) \ge \sum_{K\in\mathcal{T}_h} \Big(\nu|\boldsymbol{v_h}|^2_{H^1(K)} - 2\nu \|\boldsymbol{\partial_n v_h}\|_{\partial K} \|\Phi^{k-1}((\boldsymbol{v_h})_t - \tilde{v}_h)\|_{\partial K} + \nu \frac{\tau}{h_K} \|\Phi^{k-1}((\boldsymbol{v_h})_t - \tilde{v}_h)\|^2_{\partial K} \Big).$$

Since $\boldsymbol{v_h} \in \mathrm{BDM}^k_h$ is a piecewise polynomial, we can apply the discrete trace inequality (2.6) to the second term, followed by Young's inequality to arrive at

$$\begin{aligned} a((\boldsymbol{v_h}, \tilde{v}_h), (\boldsymbol{v_h}, \tilde{v}_h)) &\ge \sum_{K\in\mathcal{T}_h} \Big(\nu|\boldsymbol{v_h}|^2_{H^1(K)} - 2\nu \frac{C_{\max}}{\sqrt{h_K}} |\boldsymbol{v_h}|_{H^1(K)} \|\Phi^{k-1}((\boldsymbol{v_h})_t - \tilde{v}_h)\|_{\partial K} + \nu \frac{\tau}{h_K} \|\Phi^{k-1}((\boldsymbol{v_h})_t - \tilde{v}_h)\|^2_{\partial K} \Big) \\ &\ge \sum_{K\in\mathcal{T}_h} \Big(\frac{\nu}{2} |\boldsymbol{v_h}|^2_{H^1(K)} + \nu \frac{\tau - 2C^2_{\max}}{h_K} \|\Phi^{k-1}((\boldsymbol{v_h})_t - \tilde{v}_h)\|^2_{\partial K} \Big) \\ &\ge \nu C \sum_{K\in\mathcal{T}_h} \Big(|\boldsymbol{v_h}|^2_{H^1(K)} + \frac{\tau}{h_K} \|\Phi^{k-1}((\boldsymbol{v_h})_t - \tilde{v}_h)\|^2_{\partial K} \Big). \end{aligned}$$

Finally, if we suppose $\tau > 2C^2_{\max}$ and set

$$C := \min\Big\{ \frac{1}{2}, \frac{\tau - 2C^2_{\max}}{\tau} \Big\} > 0,$$

then using (3.13), we get (3.10) for $\alpha = C/(1 + C^2_{\max})$. □

The next step towards stability is proving the inf-sup condition for $b(\cdot,\cdot)$.

Lemma 3.5. *There exists $\beta > 0$ independent of h_K such that*

$$\sup_{(\boldsymbol{v_h}, \tilde{v}_h) \in \boldsymbol{V_h}} \frac{b((\boldsymbol{v_h}, \tilde{v}_h), q_h)}{|||(\boldsymbol{v_h}, \tilde{v}_h)|||} \ge \frac{\beta}{\sqrt{\nu}} \|q_h\|_\Omega \quad \textit{for all } q_h \in Q^{k-1}_h.$$

Proof. According to the Fortin criterion, see [17, Lemma 4.19], we need to prove that there exists a Fortin operator $\boldsymbol{\Pi} : [H^1(\Omega)]^2 \to \boldsymbol{V_h}$ such that for every $\boldsymbol{v} \in [H^1(\Omega)]^2$ the following conditions hold:

$$b((\boldsymbol{v}, \tilde{v}), q_h) = b(\boldsymbol{\Pi}(\boldsymbol{v}), q_h) \quad \text{for all } q_h \in Q_h^{k-1}, \tag{3.14}$$

$$|||\boldsymbol{\Pi}(\boldsymbol{v})||| \leq C\sqrt{\nu}\|\boldsymbol{v}\|_{H^1(\Omega)}. \tag{3.15}$$

Let $\boldsymbol{v} \in [H^1(\Omega)]^2$ and let us consider the operator $\boldsymbol{\Pi}(\boldsymbol{v}) := (\Pi^k(\boldsymbol{v}), \Phi^{k-1}(v_t))$. It is well known, see [2, Section 2.5], that Π^k satisfies (3.14). To prove (3.15) we denote $(\boldsymbol{w_h}, \tilde{w}_h) := \boldsymbol{\Pi}(\boldsymbol{v})$. Then using the discrete trace inequality (2.6) and the fact that the projection is a bounded operator, we get

$$\begin{aligned} |||(\boldsymbol{w_h}, \tilde{w}_h)|||^2 &= \sum_{K\in\mathcal{T}_h} \nu\Big(|\boldsymbol{w_h}|^2_{H^1(K)} + h_K\|\boldsymbol{\partial_n} \boldsymbol{w_h}\|^2_{\partial K} + \frac{\tau}{h_K}\|\Phi^{k-1}((\boldsymbol{w_h})_t - \tilde{w}_h)\|^2_{\partial K}\Big) \\ &\leq \sum_{K\in\mathcal{T}_h} \nu\Big((1 + C^2_{\max})|\boldsymbol{w_h}|^2_{H^1(K)} + \frac{\tau}{h_K}\|(\boldsymbol{w_h})_t - \tilde{w}_h\|^2_{\partial K}\Big). \end{aligned} \tag{3.16}$$

Applying the triangle inequality for the last term of (3.16), we arrive at

$$\begin{aligned} |||(\boldsymbol{w_h}, \tilde{w}_h)|||^2 &\leq \sum_{K\in\mathcal{T}_h} \nu\Big((1 + C^2_{\max})|\boldsymbol{w_h}|^2_{H^1(K)} + \frac{2\tau}{h_K}\big(\|(\boldsymbol{w_h})_t - v_t\|^2_{\partial K} + \|v_t - \tilde{w}_h\|^2_{\partial K}\big)\Big) \\ &=: \sum_{K\in\mathcal{T}_h} \nu\Big((1 + C^2_{\max})\mathfrak{T}^K_1 + \frac{2\tau}{h_K}(\mathfrak{T}^K_2 + \mathfrak{T}^K_3)\Big). \end{aligned}$$

Using the stability of Π^k leads to

$$\mathfrak{T}^K_1 = |\Pi^k(\boldsymbol{v})|^2_{H^1(K)} \leq c_1|\boldsymbol{v}|^2_{H^1(K)}. \tag{3.17}$$

Using (2.8) and the local trace inequality (2.7), we get

$$\begin{aligned} \mathfrak{T}^K_2 \leq \|\boldsymbol{v} - \boldsymbol{w_h}\|^2_{\partial K} &\leq \tilde{c}_1\Big(\frac{1}{h_K}\|\boldsymbol{v} - \boldsymbol{w_h}\|^2_K + h_K|\boldsymbol{v} - \boldsymbol{w_h}|^2_{H^1(K)}\Big) \\ &\leq \tilde{c}_1(\tilde{c}_2 h_K|\boldsymbol{v}|^2_{H^1(K)} + \tilde{c}_3 h_K|\boldsymbol{v}|^2_{H^1(K)}) \\ &\leq \tilde{c}_1(\tilde{c}_2 + \tilde{c}_3)h_K|\boldsymbol{v}|^2_{H^1(K)}. \end{aligned} \tag{3.18}$$

Finally, using the trace L^2-projection approximation (2.9) for the third term, we get

$$\mathfrak{T}^K_3 \leq \tilde{c}_4 h_K|\boldsymbol{v}|^2_{H^1(K)}. \tag{3.19}$$

Then collecting (3.17), (3.18) and (3.19), we obtain (3.15) with

$$C := \sqrt{(1 + C^2_{\max})c_1 + 2\tau\tilde{c}_1(\tilde{c}_2 + \tilde{c}_3) + 2\tau\tilde{c}_4},$$

which finishes the proof. □

Using the last two results and the standard theory of variational problems with constraints [2, Section 4.2], we deduce there exists a unique solution of (3.6). In addition, thanks to the derivation carried out in Section 3.1, method (3.6) is consistent as the following result shows.

Lemma 3.6 (Consistency). *Let $(\boldsymbol{u}, p) \in [H^1(\Omega) \cap H^2(\mathcal{T}_h)]^2 \times L^2(\Omega)$ be the solution of problem (2.4) and $\tilde{u} = u_t$ on all edges of $\mathcal{E}_h$. If $(\boldsymbol{u_h}, \tilde{u}_h, p_h) \in \boldsymbol{V_h} \times Q_h^{k-1}$ solves (3.6), then for all $(\boldsymbol{v_h}, \tilde{v}_h, q_h) \in \boldsymbol{V_h} \times Q_h^{k-1}$ the following holds:*

$$a((\boldsymbol{u} - \boldsymbol{u_h}, \tilde{u} - \tilde{u}_h), (\boldsymbol{v_h}, \tilde{v}_h)) + b((\boldsymbol{u} - \boldsymbol{u_h}, \tilde{u} - \tilde{u}_h), q_h) + b((\boldsymbol{v_h}, \tilde{v}_h), p - p_h) = 0.$$

3.3 Error Analysis

In this section, we present the error estimates for the method. These estimates are proved using the norm

$$|||(\boldsymbol{u}, \tilde{u}, p)|||_h := |||(\boldsymbol{u}, \tilde{u})||| + \frac{1}{\sqrt{\nu}}\|p\|_\Omega.$$

The first step is the following version of Cea's lemma.

Lemma 3.7. *Let $(\boldsymbol{u}, p) \in [H^1(\Omega) \cap H^2(\mathcal{T}_h)]^2 \times L^2(\Omega)$ be the solution of (2.4), $\tilde{u} = u_t$ on all edges in $\mathcal{E}_h$, and let $(\boldsymbol{u_h}, \tilde{u}_h, p_h) \in \boldsymbol{V_h} \times Q_h^{k-1}$ be the solution of (3.6). Then there exists $C > 0$, independent of h and ν, such that*

$$|||(\boldsymbol{u} - \boldsymbol{u_h}, \tilde{u} - \tilde{u}_h, p - p_h)|||_h \leq C \inf_{(\boldsymbol{v_h}, \tilde{v}_h, q_h) \in \boldsymbol{V_h} \times Q_h^{k-1}} |||(\boldsymbol{u} - \boldsymbol{v_h}, \tilde{u} - \tilde{v}_h, p - q_h)|||_h. \tag{3.20}$$

Proof. Let us denote

$$B((\boldsymbol{w_h}, \tilde{w}_h, r_h), (\boldsymbol{v_h}, \tilde{v}_h, q_h)) := a((\boldsymbol{w_h}, \tilde{w}_h), (\boldsymbol{v_h}, \tilde{v}_h)) + b((\boldsymbol{v_h}, \tilde{v}_h), r_h) + b((\boldsymbol{w_h}, \tilde{w}_h), q_h).$$

Using Lemmas 3.4 and 3.5, and [17, Proposition 2.36], we get the following stability for B: There exists $\beta_B > 0$, independent of h and ν, such that for all $(\boldsymbol{v_h}, \tilde{v}_h, q_h) \in \boldsymbol{V_h} \times Q_h^{k-1}$ there exists $(\boldsymbol{w_h}, \tilde{w}_h, r_h) \in \boldsymbol{V_h} \times Q_h^{k-1}$ such that $|||(\boldsymbol{w_h}, \tilde{w}_h, r_h)|||_h = 1$, and

$$B((\boldsymbol{v_h}, \tilde{v}_h, q_h), (\boldsymbol{w_h}, \tilde{w}_h, r_h)) \geq \beta_B |||(\boldsymbol{v_h}, \tilde{v}_h, q_h)|||_h. \tag{3.21}$$

Now Lemma 3.3 yields the following continuity for B: there exists $C_B > 0$ such that

$$|B((\boldsymbol{w_h}, \tilde{w}_h, r_h), (\boldsymbol{v_h}, \tilde{v}_h, q_h))| \leq C_B |||(\boldsymbol{w_h}, \tilde{w}_h, r_h)|||_h |||(\boldsymbol{v_h}, \tilde{v}_h, q_h)|||_h. \tag{3.22}$$

Let $(\boldsymbol{v_h}, \tilde{v}_h, q_h) \in \boldsymbol{V_h}$. Then, using Lemma 3.6, the triangle inequality, (3.21) and (3.22), we arrive at

$$\begin{aligned} |||(\boldsymbol{v_h} - \boldsymbol{u_h}, \tilde{v}_h - \tilde{u}_h, q_h - p_h)|||_h &\leq \frac{1}{\beta_B} B((\boldsymbol{v_h} - \boldsymbol{u}, \tilde{v}_h - \tilde{u}, q_h - p), (\boldsymbol{w_h}, \tilde{w}_h, r_h)) \\ &\quad + \frac{1}{\beta_B} B((\boldsymbol{u} - \boldsymbol{u_h}, \tilde{u} - \tilde{u}_h, p - p_h), (\boldsymbol{w_h}, \tilde{w}_h, r_h)) \\ &\leq \frac{C_B}{\beta_B} |||(\boldsymbol{v_h} - \boldsymbol{u}, \tilde{v}_h - \tilde{u}, q_h - p)|||_h. \end{aligned}$$

Thus, we get (3.20) with $C := 1 + C_B/\beta_B$. □

We prove the following error estimate using standard interpolation estimates.

Lemma 3.8 (HDG Error). *Let us assume $(\boldsymbol{u}, p) \in [H^1(\Omega) \cap H^{k+1}(\mathcal{T}_h)]^2 \times H^k(\mathcal{T}_h)$ is the solution of (2.4), and $\tilde{u} = u_t$ on all edges in $\mathcal{E}_h$. If $(\boldsymbol{u_h}, \tilde{u}_h, p_h) \in \boldsymbol{V_h} \times Q_h^{k-1}$ solves the discrete problem (3.6), then there exists $C > 0$, independent of h, such that*

$$|||(\boldsymbol{u} - \boldsymbol{u_h}, \tilde{u} - \tilde{u}_h, p - p_h)|||_h \leq C h^k \Big(\sqrt{\nu} \|\boldsymbol{u}\|_{H^{k+1}(\mathcal{T}_h)} + \frac{1}{\sqrt{\nu}} \|p\|_{H^k(\mathcal{T}_h)} \Big). \tag{3.23}$$

Proof. Let us consider the Fortin operator $\boldsymbol{\Pi}$ defined in the proof of Lemma 3.5. If $\boldsymbol{\Pi}(\boldsymbol{u}) = (\boldsymbol{w_h}, \tilde{w}_h)$, then by using the triangle inequality and boundedness of the projection Φ^{k-1}, we get

$$\begin{aligned} |||(\boldsymbol{u} - \boldsymbol{w_h}, \tilde{u} - \tilde{w}_h)|||^2 &= \sum_{K \in \mathcal{T}_h} \nu \Big(|\boldsymbol{u} - \boldsymbol{w_h}|^2_{H^1(K)} + h_K \|\partial_{\boldsymbol{n}}(\boldsymbol{u} - \boldsymbol{w_h})\|^2_{\partial K} + \frac{\tau}{h_K} \|\Phi^{k-1}((\boldsymbol{u} - \boldsymbol{w_h})_t - (\tilde{u} - \tilde{w}_h))\|^2_{\partial K} \Big) \\ &\leq \sum_{K \in \mathcal{T}_h} \nu \Big(|\boldsymbol{u} - \boldsymbol{w_h}|^2_{H^1(K)} + h_K \|\partial_{\boldsymbol{n}}(\boldsymbol{u} - \boldsymbol{w_h})\|^2_{\partial K} + \frac{2c_1\tau}{h_K} (\|\boldsymbol{u} - \boldsymbol{w_h}\|^2_{\partial K} + \|\tilde{u} - \tilde{w}_h\|^2_{\partial K}) \Big) \\ &=: \sum_{K \in \mathcal{T}_h} \nu \Big(\mathfrak{T}_1^K + h_K \mathfrak{T}_2^K + \frac{2c_1\tau}{h_K} (\mathfrak{T}_3^K + \mathfrak{T}_4^K) \Big). \end{aligned} \tag{3.24}$$

For the first term from (3.24), we use the BDM approximation (2.8) to get

$$\mathfrak{T}_1^K \leq c_2 h_K^{2k} |\boldsymbol{u}|^2_{H^{k+1}(K)}. \tag{3.25}$$

Next we use the local trace inequality (2.7) to get

$$\mathfrak{T}_2^K \leq c_3 \Big(\frac{1}{h_K} |\boldsymbol{u} - \boldsymbol{w_h}|^2_{H^1(K)} + h_K |\boldsymbol{u} - \boldsymbol{w_h}|^2_{H^2(K)} \Big). \tag{3.26}$$

Let $\mathcal{L}^k\boldsymbol{u}$ be the usual Lagrange interpolant of degree k of $\boldsymbol{u}$ (see [17, Example 1.31]). Using the triangle inequality followed by the local inverse inequality (2.5), the local Lagrange approximation [17, Example 1.106] and (2.8), we see that (3.26) becomes

$$\begin{aligned}\mathfrak{T}_2^K &\le c_3\Big(\frac{1}{h_K}|\boldsymbol{u}-\boldsymbol{w_h}|^2_{H^1(K)} + 2h_K|\boldsymbol{u}-\mathcal{L}^k\boldsymbol{u}|^2_{H^2(K)} + 2h_K|\mathcal{L}^k\boldsymbol{u}-\boldsymbol{w_h}|^2_{H^2(K)}\Big)\\ &\le c_3\Big((c_4+2c_5)h_K^{2k-1}|\boldsymbol{u}|^2_{H^{k+1}(K)} + \frac{2c_6}{h_K}|\mathcal{L}^k\boldsymbol{u}-\boldsymbol{w_h}|^2_{H^1(K)}\Big)\\ &\le c_3\Big((c_4+2c_5)h_K^{2k-1}|\boldsymbol{u}|^2_{H^{k+1}(K)} + \frac{4c_6}{h_K}|\mathcal{L}^k\boldsymbol{u}-\boldsymbol{u}|^2_{H^1(K)} + \frac{4c_6}{h_K}|\boldsymbol{u}-\boldsymbol{w_h}|^2_{H^1(K)}\Big)\\ &\le c_3(c_4+2c_5+4c_6(c_7+c_8))h_K^{2k-1}|\boldsymbol{u}|^2_{H^{k+1}(K)}. \end{aligned} \tag{3.27}$$

For the third term in (3.24), we use (2.7) and (2.8) to get

$$\mathfrak{T}_3^K \le c_9\Big(\frac{1}{h_K}\|\boldsymbol{u}-\boldsymbol{w_h}\|^2_K + h_K|\boldsymbol{u}-\boldsymbol{w_h}|^2_{H^1(K)}\Big) \le c_9c_{10}h_K^{2k+1}|\boldsymbol{u}|^2_{H^{k+1}(K)}. \tag{3.28}$$

The last term in (3.24) is bounded using (2.9) as follows:

$$\mathfrak{T}_4^K \le c_{11}h_K^{2k+1}|\boldsymbol{u}|^2_{H^{k+1}(K)}. \tag{3.29}$$

Finally, the local L^2-projection approximation (2.10) gives

$$\inf_{q\in Q_h^{k-1}}\|p-q_h\|_\Omega = \|p-\Psi_h^{k-1}(p)\|_\Omega \le \tilde{c}_1h_K^k\|p\|_{H^k(\mathcal{T}_h)}. \tag{3.30}$$

Thus, putting together (3.24) with (3.25), (3.27)–(3.30), and using the shape regularity of the mesh, we get

$$\inf_{(\boldsymbol{v_h},\tilde{v}_h,q_h)\in\boldsymbol{V_h}}|||(\boldsymbol{u}-\boldsymbol{v_h},\tilde{u}-\tilde{v}_h,p-q_h)|||_h \le \hat{C}h^k\Big(\sqrt{\nu}\|\boldsymbol{u}\|_{H^{k+1}(\mathcal{T}_h)} + \frac{1}{\sqrt{\nu}}\|p\|_{H^k(\mathcal{T}_h)}\Big)$$

with

$$\hat{C} := \max\Big\{\sqrt{c_2+c_3(c_4+2c_5+4c_6(c_7+c_8))+2\tau c_1c_9c_{10}+2\tau c_1c_{11}},\,\tilde{c}_1\Big\},$$

and the result (3.23) follows from Lemma 3.7. □

3.4 NVTF Boundary Conditions

As we mentioned before, the analysis in case of NVTF boundary conditions (2.3) is similar. Thus, we just highlight the main differences. If we consider NVTF boundary conditions (2.3), then to discretise the velocity we use the BDM space

$$\mathrm{BDM}^k_{h,0} := \{\boldsymbol{v_h}\in\mathrm{BDM}^k_h : (\boldsymbol{v_h})_n = 0 \text{ on } \Gamma\}.$$

For the Lagrange multiplier we use the polynomial space M_h^{k-1}, while the pressure is discretised using

$$Q^{k-1}_{h,0} := \Big\{q_h\in Q_h^{k-1} : \int_\Omega q_h\,d\boldsymbol{x} = 0\Big\}.$$

The product space then becomes $\boldsymbol{V_h} := \mathrm{BDM}^k_{h,0}\times M_h^{k-1}$ and we pose the following discrete problem:

Find $(\boldsymbol{u_h},\tilde{u}_h,p_h)\in\boldsymbol{V_h}\times Q^{k-1}_{h,0}$ such that for all $(\boldsymbol{v_h},\tilde{v}_h,q_h)\in\boldsymbol{V_h}\times Q^{k-1}_{h,0}$,

$$\begin{cases} a((\boldsymbol{u_h},\tilde{u}_h),(\boldsymbol{v_h},\tilde{v}_h)) + b((\boldsymbol{v_h},\tilde{v}_h),p_h) = \displaystyle\int_\Omega \boldsymbol{f}\boldsymbol{v_h}\,d\boldsymbol{x} + \int_\Gamma g\tilde{v}_h\,ds,\\ b((\boldsymbol{u_h},\tilde{u}_h),q_h) = 0. \end{cases} \tag{3.31}$$

In obtaining (3.31) the only difference step in the derivation is that now (3.4) is replaced by

$$\int_\Omega(-\nu\Delta\boldsymbol{u}+\nabla p)\cdot\boldsymbol{v_h}\,d\boldsymbol{x} = \sum_{K\in\mathcal{T}_h}\Big(\int_K \nu\nabla\boldsymbol{u}:\nabla\boldsymbol{v_h}\,d\boldsymbol{x} - \int_K p\nabla\cdot\boldsymbol{v_h}\,d\boldsymbol{x} - \int_{\partial K}\sigma_{nt}((\boldsymbol{v_h})_t-\tilde{v}_h)\,ds\Big) - \int_\Gamma g\tilde{v}_h\,ds.$$

Concerning the analysis, the proofs of all the results presented in the last sections remain essentially unchanged.

4 The Domain Decomposition Preconditioner

Let us assume that we have to solve the linear system

$$\mathbf{A}\boldsymbol{U} = \boldsymbol{F},$$

where $\mathbf{A}$ is the matrix arising from discretisation of the Stokes equations on the domain Ω, $\boldsymbol{U}$ is the vector of unknowns and $\boldsymbol{F}$ is the right-hand side. To accelerate the performance of an iterative Krylov method applied to this system we will consider domain decomposition preconditioners which are naturally parallel [12, Chapter 3]. They are based on an overlapping partition of the computational domain.

Let $\{\mathcal{T}_{h,i}\}_{i=1}^N$ be a partition of the triangulation $\mathcal{T}_h$. For an integer value $l \geq 0$, we define an overlapping decomposition $\{\mathcal{T}_{h,i}^l\}_{i=1}^N$ such that $\mathcal{T}_{h,i}^l$ is a set of all triangles from $\mathcal{T}_{h,i}^{l-1}$ and all triangles from $\mathcal{T}_h \setminus \mathcal{T}_{h,i}^{l-1}$ that have non-empty intersection with $\mathcal{T}_{h,i}^{l-1}$, and $\mathcal{T}_{h,i}^0 = \mathcal{T}_{h,i}$. With this definition the width of the overlap will be $2l$. Furthermore, if W_h stands for the finite element space associated to $\mathcal{T}_h$, then $W_{h,i}^l$ is the local finite element space on $\mathcal{T}_{h,i}^l$ that is a triangulation of Ω_i.

Let $\mathcal{N}$ be the set of indices of degrees of freedom of W_h and let $\mathcal{N}_i^l$ be the set of indices of degrees of freedom of $W_{h,i}^l$ for $l \geq 0$. Moreover, we define the restriction operator $\mathbf{R}_i : W_h \to W_{h,i}^l$ as a rectangular matrix $|\mathcal{N}_i^l| \times |\mathcal{N}|$ such that if $\boldsymbol{V}$ is the vector of degrees of freedom of $v_h \in W_h$, then $\mathbf{R}_i\boldsymbol{V}$ is the vector of degrees of freedom of $W_{h,i}^l$ in Ω_i. Abusing notation, we denote by $\mathbf{R}_i$ both the operator and its associated matrix. The extension operator from $W_{h,i}^l$ to W_h and its associated matrix are both given by $\mathbf{R}_i^T$. In addition, we introduce a partition of unity $\mathbf{D}_i$ as a diagonal matrix $|\mathcal{N}_i^l| \times |\mathcal{N}_i^l|$ such that

$$\mathbf{Id} = \sum_{i=1}^N \mathbf{R}_i^T \mathbf{D}_i \mathbf{R}_i,$$

where $\mathbf{Id} \in \mathbb{R}^{|\mathcal{N}|\times|\mathcal{N}|}$ is the identity matrix.

We are ready to present the first preconditioner, called Restricted Additive Schwarz (RAS) [3], given by

$$\mathbf{M}_{\mathrm{RAS}}^{-1} = \sum_{i=1}^N \mathbf{R}_i^T \mathbf{D}_i (\mathbf{R}_i \mathbf{A} \mathbf{R}_i^T)^{-1} \mathbf{R}_i. \tag{4.1}$$

We also introduce a new preconditioner that is a modification of the above one. The modification is similar to the Optimized RAS [30], however we do not use Robin IC. For this, let $\mathbf{B}_i$ be the matrix associated to a discretisation of (2.1) in Ω_i where we impose either TVNF (2.2) or NVTF (2.3) boundary conditions in Ω_i. Then, the preconditioner reads

$$\mathbf{M}_{\mathrm{MRAS}}^{-1} = \sum_{i=1}^N \mathbf{R}_i^T \mathbf{D}_i \mathbf{B}_i^{-1} \mathbf{R}_i. \tag{4.2}$$

Remark 4.1. The improvement of convergence in the case of Optimized RAS depends on the choice of the parameter. This parameter depends on the problem and discretisation. The big advantage of MRAS preconditioners is that they are parameter-free.

4.1 Partition of Unity

The above definitions of the preconditioners can be associated with any discretisation of the problem. However, each discretisation involves the construction of a relevant partition of unity $\mathbf{D}_i$, $i = 1, \ldots, N$. We discuss here the construction of $\mathbf{D}_i$ when the problem (2.1) is discretised by the HDG method in case $k = 1$, either with TVNF boundary conditions (3.6), or NVTF boundary conditions (3.31). Let us introduce the piecewise linear functions $\tilde{\chi}_i^l$ of $\mathcal{T}_h$ such that

$$\tilde{\chi}_i^l = \begin{cases} 1 & \text{on all nodes of } \mathcal{T}_{h,i}^0, \\ 0 & \text{on other nodes.} \end{cases}$$

Now we define the piecewise linear functions χ_i^l of $\mathcal{T}_{h,i}^l$ as follows:

$$\chi_i^l := \frac{\tilde{\chi}_i^l}{\sum_{j=1}^N \tilde{\chi}_j^l}.$$

Obviously $\sum_{i=1}^N \chi_i^l = 1$. We define the partition of unity matrix $\mathbf{D}_i$ as a block diagonal matrix where the first block $\mathbf{D}_i^{\mathrm{BDM}}$ is associated with BDM_h^1, the second block $\mathbf{D}_i^M$ with M_h^0, and the third block $\mathbf{D}_i^Q$ with Q_h^0. The degrees of freedom of the BDM elements are associated with the normal components on the edges of the mesh. For these finite elements, the diagonal of $\mathbf{D}_i^{\mathrm{BDM}}$ is a vector obtained by interpolating χ_i^l at the two points of the edges. The degrees of freedom of the Lagrange multiplier finite elements are associated with the edges of the mesh. For these finite elements, the diagonal of $\mathbf{D}_i^M$ is a vector obtained by interpolating χ_i^l at the midpoints of the edges. For pressure finite elements, the diagonal of $\mathbf{D}_i^Q$ is a vector obtained by interpolating χ_i^l at the midpoints of the elements.

5 Numerical Results

In this section, we present a series of numerical experiments aimed at confirming the theory developed in Section 3, and to give a computational comparison of the preconditioners discussed in the previous section. All experiments have been made by using FreeFem++ [20], which is a free software specialised in variational discretisations of partial differential equations.

5.1 Convergence Validation

The computational domain for both test cases considered here is the unit square $\Omega = (0, 1)^2$. We present the results for $k = 1$, that is, the discrete space is given by $\mathrm{BDM}_h^1 \times M_{h,0}^0 \times Q_h^0$ for TVNF boundary conditions and $\mathrm{BDM}_{h,0}^1 \times M_h^0 \times Q_{h,0}^0$ for NVTF boundary conditions. We test both the symmetric method ($\varepsilon = -1$) and the non-symmetric method ($\varepsilon = 1$). For both cases we have followed the recommendation given in [21, Section 2.5.2] and taken $\tau = 6$.

The first example aims at verifying the formulation with TVNF boundary conditions (3.6). We choose the right-hand side $\boldsymbol{f}$ and the boundary datum g such that the exact solution is given by

$$\boldsymbol{u} = \mathrm{curl}\big[100(1 - \cos((1-x)^2))\sin(x^2)\sin(y^2)(1 - \cos((1-y)^2))\big], \quad p = \tan(xy).$$

In Figures 1a and 1b we show the results of the usual convergence order tests for the symmetric case and the non-symmetric case by plotting in log-log scale the error as a function of the size of the mesh. We notice that they validate the theory from Section 3.3. In addition, an optimal h^2 convergence rate is observed for $\|\boldsymbol{u} - \boldsymbol{u_h}\|_\Omega$. The proof of this last fact is lacking. This is due to the lack of regularity results concerning the solution of the continuous problem with these nonstandard boundary conditions, and hence the usual Aubin–Nitsche approach can not be advocated.

In the second example we want to verify the formulation with NVTF boundary conditions (3.31). In this case, the right-hand side $\boldsymbol{f}$ and the boundary datum g are chosen for the following exact solution:

$$\boldsymbol{u} = \mathrm{curl}\big[x^2(1-x)^2y^2(1-y)^2\big], \quad p = x^2 - y^2.$$

The convergence error with respect to the size of the mesh is depicted on the log-log plots for the symmetric case and the non-symmetric case in Figures 2a and 2b, respectively. We can see that they not only validate the theory from Section 3.3, but also show an optimal h^2 convergence rate for $\|\boldsymbol{u} - \boldsymbol{u_h}\|_\Omega$.

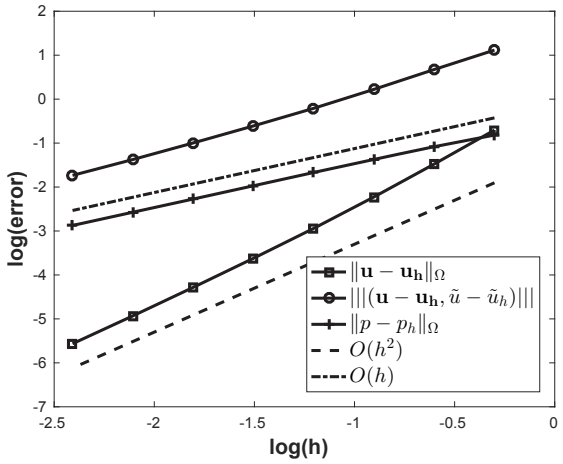

(a) Symmetric bilinear form ($\varepsilon = -1$)

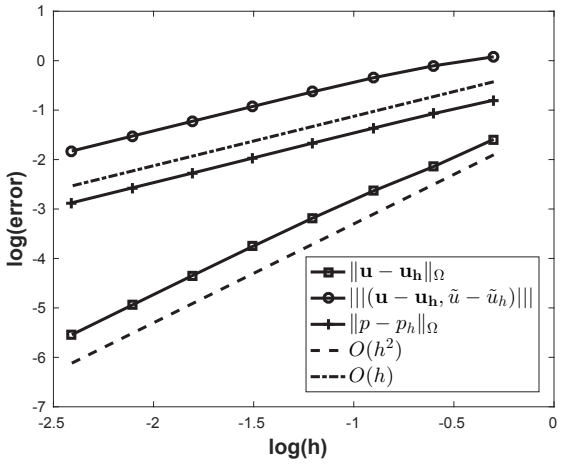

(b) Non-symmetric bilinear form ($\varepsilon = 1$)

Figure 1: Error convergence of the HDG method with TVNF boundary condition – the first example.

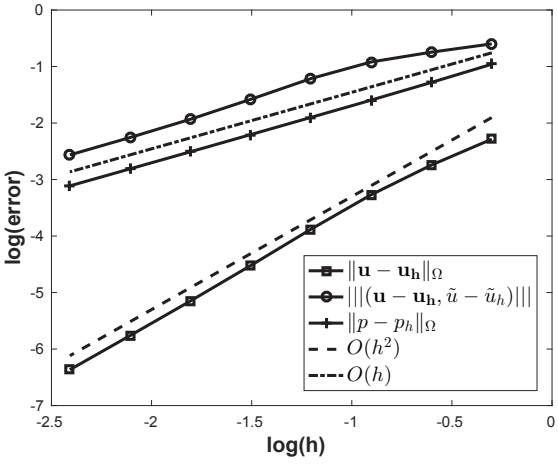

(a) Symmetric bilinear form ($\varepsilon = -1$)

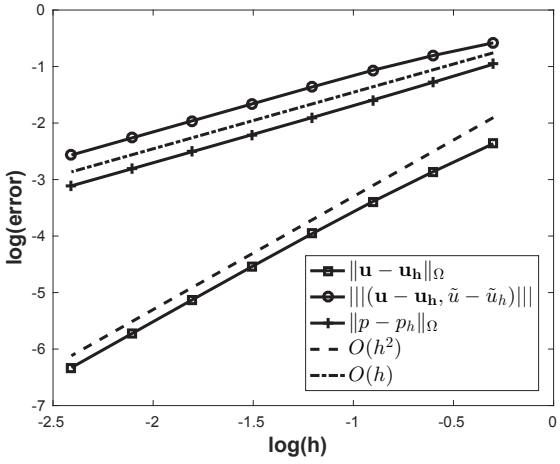

(b) Non-symmetric bilinear form ($\varepsilon = 1$)

Figure 2: Error convergence of the HDG method with NVTF boundary condition – the second example.

5.2 Comparison of Different Domain Decomposition Preconditioners

In this section, we compare the standard RAS preconditioner (4.1) with the newly introduced preconditioners, that is, the ones based on nonstandard IC. We call them MRAS preconditioners (4.2) and more precisely TVNF-MRAS for which $\mathbf{B}_i$ is the matrix arising from the discretisation of (2.1) in Ω_i with IC (2.2) on $\partial\Omega_i$, and NVTF-MRAS for which $\mathbf{B}_i$ is the matrix arising from the discretisation of (2.1) in Ω_i with IC (2.3) on $\partial\Omega_i$. As we mentioned before, our preconditioners do not depend on the used discretisation, that is why we add also similar preconditioners but based on a more standard discretisation, that is, the lowest order Taylor–Hood discretisation [18, Section II.4.2]. In all cases, they are used in conjunction with a Krylov iterative solver such as GMRES [26]. In addition, N stands for the number of subdomains. In all tables we present the number of iterations needed to achieve an euclidean norm of the error (with respect to the one domain solution) smaller than 10^{-6}. We have implemented the RAS preconditioner (4.1) and the MRAS (4.2), using both TVNF and NVTF interface conditions.

We start with the second example from the previous section. However, now we consider the symmetric ($\varepsilon = -1$) formulation with TVNF boundary conditions (3.6). The mesh is uniform and contains 125 000 triangles for a total of 565 003 degrees of freedom for the Taylor–Hood discretisation and 689 000 degrees of freedom for the HDG discretisation. We use a random initial guess for the GMRES iterative solver. The over-

	Taylor–Hood						HDG					
N	RAS		NVTF-MRAS		TVNF-MRAS		RAS		NVTF-MRAS		TVNF-MRAS	
	Unif	MTS	Unif	MTS	Unif	MTS	Unif	MTS	Unif	MTS	Unif	MTS
4	133	311	40	39	37	37	58	95	41	45	53	50
9	336	563	58	58	52	60	94	131	62	66	69	81
16	315	691	60	76	59	73	101	151	68	85	80	100
25	427	774	76	93	71	90	127	186	77	100	103	119
64	630	1132	113	147	112	132	196	280	126	172	148	183
100	769	1246	136	174	132	169	247	348	151	205	175	228
144	929	1434	158	201	155	192	306	408	178	228	192	259
196	1000	1637	180	239	168	224	354	480	198	326	212	299
256	1133	1805	201	265	183	286	403	536	226	358	233	341

Table 1: Preconditioners comparison – the first test case.

	Taylor–Hood						HDG					
N	RAS		NVTF-MRAS		TVNF-MRAS		RAS		NVTF-MRAS		TVNF-MRAS	
	Unif	MTS	Unif	MTS	Unif	MTS	Unif	MTS	Unif	MTS	Unif	MTS
4	117	220	36	39	38	36	58	95	39	47	54	48
9	294	421	63	60	54	54	103	129	66	67	77	78
16	236	510	59	73	61	68	98	153	65	83	74	94
25	300	642	68	89	72	83	120	184	77	103	88	115
64	454	916	102	144	100	122	188	279	117	160	120	165
100	559	1088	122	173	116	154	225	349	140	198	138	215
144	940	1251	176	195	145	215	342	395	198	231	183	232
196	781	1346	166	230	146	242	325	486	191	277	173	284
256	881	1553	189	269	159	272	368	538	210	316	195	309

Table 2: Preconditioners comparison – the Poiseuille problem.

lapping decomposition into subdomains can be uniform (Unif) or generated by METIS (MTS) and it has two layers of size h in the overlap.

The first thing that we can notice from Table 1 is the important convergence improvement in case of RAS applied to a system resulting from a HDG discretisation in comparison to the RAS applied to the system resulting from the Taylor–Hood discretisation despite the fact that the number of degrees of freedom is slightly bigger in the first case. The change in discretisation presumably leads to better conditioned systems to solve. Also the MRAS preconditioner with both discretisations performs better than the standard RAS method which fully justifies the use of the new IC no matter the discretisation method. Moreover, as expected, the number of iterations increases with respect to the number of the subdomains and this behaviour is common to the three preconditioners. It is worth noticing that this increase is slower than the expected linear one.

We also plot the convergence of the error for the different discretisations in Figure 3. We observe that in all cases the MRAS preconditioner (4.2) shortens the plateau region in the convergence curves significantly which leads, automatically, to an important reduction in the number of iterations.

Now we consider the Poiseuille problem and we choose the right-hand side $\boldsymbol{f}$ and the TVNF boundary condition such that the exact solution is given by

$$\boldsymbol{u} = [4y(1-y), 0]^T, \quad p = 4 - 8x.$$

We use the same mesh as in the previous case and a random initial guess for the GMRES iterative solver, but this time the overlapping decomposition has three layers of size h in the overlap.

The conclusions stay the same as in previous example since the results from Table 2 are similar to the previous ones. We consider a different problem, however on the same mesh. Hence the global matrix is the

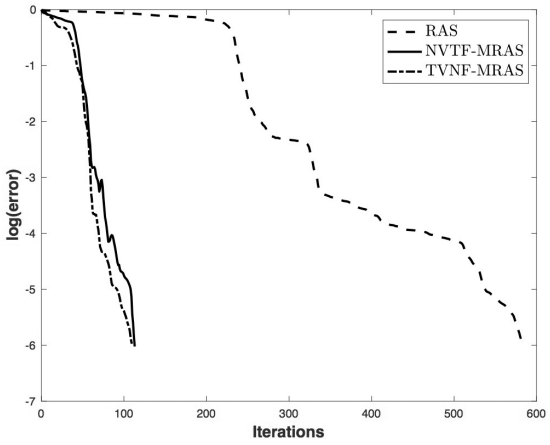

(a) Taylor–Hood, uniform decomposition

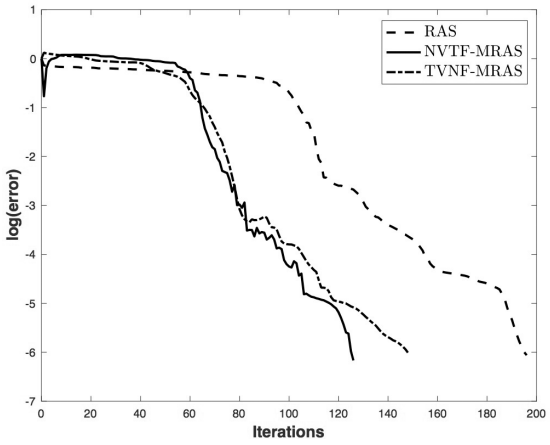

(b) HDG, uniform decomposition

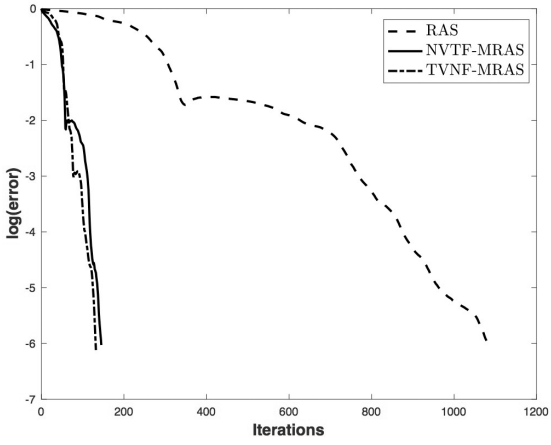

(c) Taylor–Hood, METIS decomposition

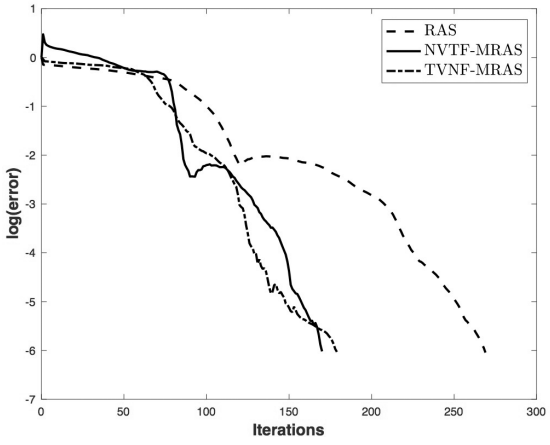

(d) HDG, METIS decomposition

Figure 3: Convergence of error in the 64 subdomains case – the first test case.

same in both cases. Thus, we can notice a reduction in the number of iterations caused by the increase of the width of the overlap.

We observe in Figure 4 that once again the MRAS preconditioner (4.2) leads to a reduction of the number of iterations in all cases.

The last example is on a T-shaped domain $\Omega = (0, 1.5) \times (0, 1) \cup (0.5, 1) \times (-1, 1)$, and we impose mixed boundary conditions given by

$$\begin{cases} \boldsymbol{u}(x, y) = (4y(1 - y), 0)^T & \text{if } x = 0, \\ \sigma_{nn}(x, y) = 0, \quad u_t(x, y) = 0 & \text{if } x = 1.5, \\ \boldsymbol{u}(x, y) = (0, 0)^T & \text{otherwise.} \end{cases}$$

In Figure 5 we plot the numerical solution obtained with the HDG discretisation using $\tau = 6$ on a coarse mesh. In this case, we used a mesh containing 379 402 triangles, which gives linear systems of a size 1 712 352 for the Taylor–Hood discretisation and 2 089 735 for the HDG discretisation. The initial guess in the GMRES iterative solver is zero. The overlapping decomposition into subdomains is generated by METIS and it has two layers of size h in the overlap.

According to Table 3 the conclusions remain the same, that is, the standard RAS method performs far better when applied to a HDG discretisation with respect to a Taylor–Hood one and the MRAS preconditioners are better than the standard RAS preconditioner for both discretisations. Figure 6 again confirms the superiority of the MRAS preconditioner over the RAS preconditioner.

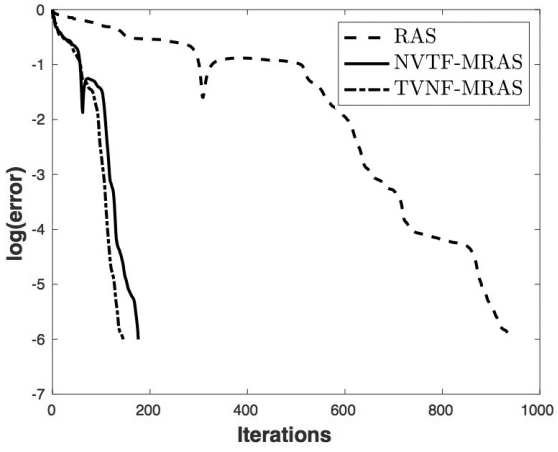

(a) Taylor–Hood, uniform decomposition

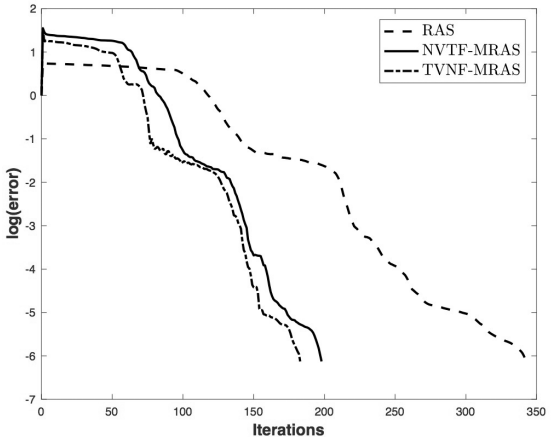

(b) HDG, uniform decomposition

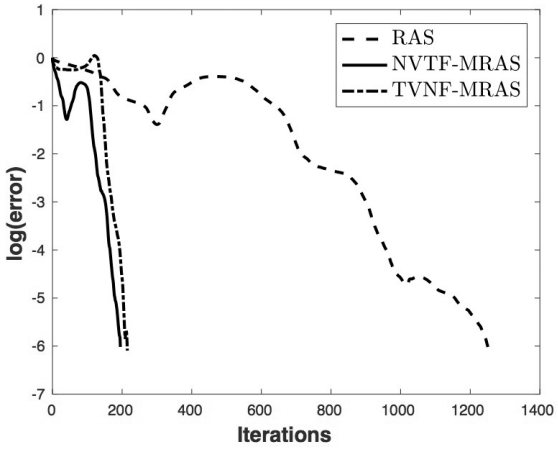

(c) Taylor–Hood, METIS decomposition

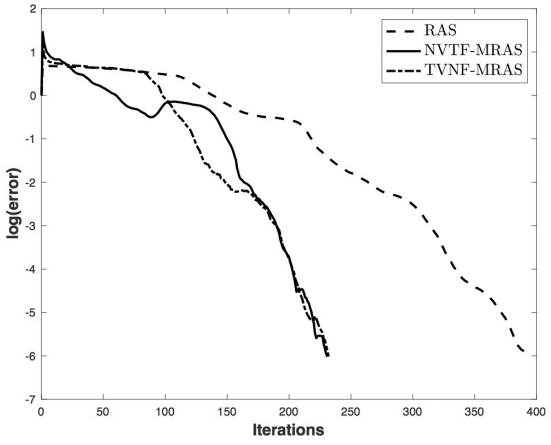

(d) HDG, METIS decomposition

Figure 4: Convergence of error in the 144 subdomains case – the Poiseuille problem.

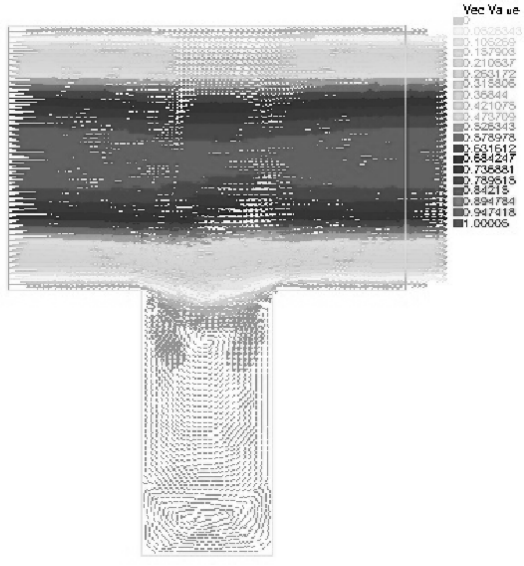

(a) Velocity field $\boldsymbol{u}$

(b) Pressure p

Figure 5: Numerical solution of the T-shaped domain problem.

	Taylor–Hood			HDG		
N	RAS	NVTF-MRAS	TVNF-MRAS	RAS	NVTF-MRAS	TVNF-MRAS
50	752	121	105	209	132	135
100	903	175	147	307	190	197
200	1272	245	211	441	264	281
400	1747	341	342	613	366	399
800	2433	469	417	863	650	549

Table 3: Preconditioners comparison – the T-shaped domain problem.

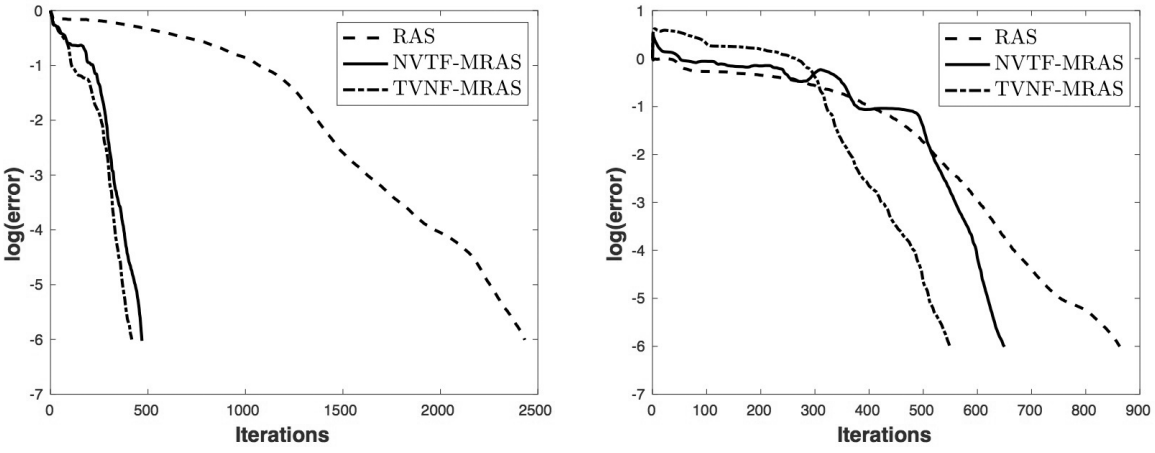

(a) Taylor–Hood **(b)** HDG

Figure 6: Convergence of error for METIS decomposition in the 800 subdomains case – the T-shaped domain problem.

6 Conclusion

In this paper, we introduced a HDG method for the Stokes equations that naturally discretises nonstandard boundary value problems such as those with TVNF and NVTF boundary conditions. This approach can be extended naturally to the case of incompressible, or nearly incompressible, elasticity. We proved the well-posedness and convergence with respect to the norm (3.7) of this method and in the numerical experiments from Section 5.1 we validated the theory and observed the optimal convergence.

To solve the discretised problem we introduced two different kinds of preconditioners with nonstandard boundary conditions whose optimality has been proved by algebraic techniques. We compared the newly introduced preconditioners to the more standard RAS preconditioner and numerical tests from Section 5.2 clearly show their superiority for different test cases in two space dimensions. Moreover, our numerical experience seems to hint that the linear systems arising from the HDG discretisation are better conditioned than those obtained using the Taylor–Hood element. This can be seen from the fact that the RAS preconditioner already performs far better when applied to the HDG method than when using Taylor–Hood.

We observed, as expected, that the Schwarz preconditioners are not scalable with respect to the number of subdomains. However, this can be fixed by using an appropriate coarse spaces [12, Chapter 4]. A suitable choice of a coarse space will be a subject of future research.

Acknowledgment: We thank Frédéric Hecht from Laboratory J. L. Lions for comments that greatly improved the FreeFem++ codes.

Funding: This research has been partially funded by the Engineering and Physical Sciences Research Council of Great Britain under the Centre for Numerical Algorithms and Intelligent Software (NAIS) for the evolving HPC platform grant EP/G036136/1.

References

[1] B. Ayuso de Dios, F. Brezzi, L. D. Marini, J. Xu and L. Zikatanov, A simple preconditioner for a discontinuous Galerkin method for the Stokes problem, *J. Sci. Comput.* **58** (2014), no. 3, 517–547.
[2] D. Boffi, F. Brezzi and M. Fortin, *Mixed Finite Element Methods and Applications*, Springer Ser. Comput. Math. 44, Springer, Heidelberg, 2013.
[3] X.-C. Cai and M. Sarkis, A restricted additive Schwarz preconditioner for general sparse linear systems, *SIAM J. Sci. Comput.* **21** (1999), no. 2, 792–797.
[4] T. Cluzeau, V. Dolean, F. Nataf and A. Quadrat, Preconditionning techniques for systems of partial differential equations based on algebraic methods, Technical Report 7953, INRIA, 2012, http://hal.inria.fr/hal-00694468.
[5] T. Cluzeau, V. Dolean, F. Nataf and A. Quadrat, Symbolic techniques for domain decomposition methods, in: *Domain Decomposition Methods in Science and Engineering XX*, Springer, Berlin (2013), 27–38.
[6] B. Cockburn, D. A. Di Pietro and A. Ern, Bridging the hybrid high-order and hybridizable discontinuous Galerkin methods, *ESAIM Math. Model. Numer. Anal.* **50** (2016), no. 3, 635–650.
[7] B. Cockburn and J. Gopalakrishnan, The derivation of hybridizable discontinuous Galerkin methods for Stokes flow, *SIAM J. Numer. Anal.* **47** (2009), no. 2, 1092–1125.
[8] B. Cockburn, J. Gopalakrishnan and R. Lazarov, Unified hybridization of discontinuous Galerkin, mixed, and continuous Galerkin methods for second order elliptic problems, *SIAM J. Numer. Anal.* **47** (2009), no. 2, 1319–1365.
[9] B. Cockburn, J. Gopalakrishnan, N. C. Nguyen, J. Peraire and F. J. Sayas, Analysis of HDG methods for Stokes flow, *Math. Comp.* **80** (2011), no. 274, 723–760.
[10] D. A. Di Pietro and A. Ern, *Mathematical Aspects of Discontinuous Galerkin Methods*, Math. Appl. (Berlin) 69, Springer, Heidelberg, 2012.
[11] D. A. Di Pietro and A. Ern, A hybrid high-order locking-free method for linear elasticity on general meshes, *Comput. Methods Appl. Mech. Engrg.* **283** (2015), 1–21.
[12] V. Dolean, P. Jolivet and F. Nataf, *An Introduction to Domain Decomposition Methods. Algorithms, Theory, and Parallel Implementation*, Society for Industrial and Applied Mathematics, Philadelphia, 2015.
[13] V. Dolean and F. Nataf, A new domain decomposition method for the compressible Euler equations, *ESAIM Math. Model. Numer. Anal.* **40** (2006), no. 4, 689–703.
[14] V. Dolean, F. Nataf and F. Rapin, Deriving a new domain decomposition method for the Stokes equations using the Smith factorization, *Math. Comp.* **78** (2009), no. 266, 789–814.
[15] H. Egger and C. Waluga, A hybrid discontinuous Galerkin method for Darcy–Stokes problems, in: *Domain Decomposition Methods in Science and Engineering XX*, Lect. Notes Comput. Sci. Eng. 91, Springer, Berlin (2013), 663–670.
[16] H. Egger and C. Waluga, *hp* analysis of a hybrid DG method for Stokes flow, *IMA J. Numer. Anal.* **33** (2013), no. 2, 687–721.
[17] A. Ern and J. L. Guermond, *Theory and Practice of Finite Elements*, Appl. Math. Sci. 159, Springer, New York, 2004.
[18] V. Girault and P. A. Raviart, *Finite Element Methods for Navier–Stokes Equations. Theory and Algorithms*, Springer Ser. Comput. Math. 5, Springer, Berlin, 1986.
[19] P. Gosselet and C. Rey, Non-overlapping domain decomposition methods in structural mechanics, *Arch. Comput. Methods Eng.* **13** (2006), no. 4, 515–572.
[20] F. Hecht, New development in FreeFem++, *J. Numer. Math.* **20** (2012), no. 3–4, 251–265.
[21] C. Lehrenfeld, *Hybrid discontinuous Galerkin methods for solving incompressible flow problems*, Dissertation, Rheinisch-Westfälischen Technischen Hochschule Aachen, 2010.
[22] C. Lehrenfeld and J. Schöberl, High order exactly divergence-free hybrid discontinuous Galerkin methods for unsteady incompressible flows, *Comput. Methods Appl. Mech. Engrg.* **307** (2016), 339–361.
[23] I. Oikawa, Analysis of a reduced-order HDG method for the Stokes equations, *J. Sci. Comput.* **67** (2016), no. 2, 475–492.
[24] A. Quarteroni and A. Valli, *Domain Decomposition Methods for Partial Differential Equations*, Clarendon Press, Oxford, 1999.
[25] W. H. Reed and T. R. Hill, Triangular mesh methods for the neutron transport for a scalar hyperbolic equation, Technical Report LA-UR-73-479, Los Alamos Scientific Laboratory, 1973.
[26] Y. Saad and M. H. Schultz, GMRES: A generalized minimal residual algorithm for solving nonsymmetric linear systems, *SIAM J. Sci. Statist. Comput.* **7** (1986), no. 3, 856–869.
[27] D. Schötzau, C. Schwab and A. Toselli, Mixed *hp*-DGFEM for incompressible flows, *SIAM J. Numer. Anal.* **40** (2002), no. 6, 2171–2194.

[28] B. F. Smith, P. E. Bjørstad and W. Gropp, *Domain Decomposition: Parallel Multilevel Methods for Elliptic Partial Differential Equations*, Cambridge University Press, Cambridge, 1996.
[29] H. J. S. Smith, On systems of linear indeterminate equations and congruences, *Philos. Trans. A* **151** (1861), 293–326.
[30] A. St-Cyr, M. J. Gander and S. J. Thomas, Optimized multiplicative, additive, and restricted additive Schwarz preconditioning, *SIAM J. Sci. Comput.* **29** (2007), no. 6, 2402–2425.
[31] A. Toselli and O. Widlund, *Domain Decomposition Methods – Algorithms and Theory*, Springer Ser. Comput. Math. 34, Springer, Berlin, 2005.